AD-A078 430 SALFORD UNIV (ENGLAND) DEPT OF PURE AND APPLIED PHYSICS F/G 20/12
SCANNING TRANSMISSION ELECTRON MICROSCOPY OF ELECTROMAGNETIC ST--ETC(U)
OCT 79 R S TEBBLE AFOSR-76-2896

UNCLASSIFIED AFOSR-TR-79-1265 NL

| OF |
AD-
A 078430

END
DATE
FILMED
1-80
DDC

LEVEL II

Contract/Grant Number AFOSR 76 - 2896

Scanning transmission electron microscopy of electromagnetic structure

Robert S Tebble
Department of Physics
University
Salford M5 4WT

21st October 1979

Final Scientific Report 1978 October 01 - 1979 September 30

Approved for public release: distribution unlimited

Prepared for Air Force Office of Scientific Research, Bolling AFB,
Building 410, Washington, DC 20332

and

EUROPEAN OFFICE OF AEROSPACE RESEARCH AND DEVELOPMENT
London, England

Unclassified

1. Report Number	2. Govt Accession No.	3. Recipient's Catalog Number
AFOSR-TR-79-1265	(18) AFOSR	(19) TR-79-1265

4. Title (and Subtitle)	5. Type of Report & Period Covered
(6) Scanning transmission electron microscopy of electromagnetic structure	Final Report 1978 October 1 - 1979 Sept 30
	6. Performing Org. Report Number

7. Author(s)	8. Contract or Grant Number
(10) Robert S. Tebble (12) 39	(15) AFOSR-76-2896

9. Performing Organization Name and Address	10. Program Element, Project, Task Area & Work Unit Numbers
Department of Pure and Applied Physics University of Salford Salford M4 5WT, England	P.E. 61102F P/Task (16) 2306/B2 (17) B2

11. Controlling Office Name and Address	12. Report Date
Air Force Office of Scientific Research /NE (11) Bolling AFB, Washington DC 20332	21 Oct [redacted] 79 13. Number of Pages 36

14. Monitoring Agency Name and Address	15.
405 006	UNCLASSIFIED

16. & 17. Distribution Statement

Approved for public release; distribution unlimited.

18. Supplementary Notes

(9) Final rept. 1 Oct 78-30 Sep 79.

19. Key Words

Amorphous alloys, FeB, Lorentz electron microscopy; magnetic domains

20. Abstract

The report describes the application of Lorentz electron microscopy to the study of structural changes of amorphous alloys in composition region ~ $Fe_{80}B_{20}$. Significant changes in the magnetic domain structure can in certain instances be associated with phase transitions, segregation and stress effects together with changes in the amorphicity. The appearance of magnetization ripple and the formation of regular stripe domain patterns are examples of the magnetic structures which can be observed by defocussing the electron microscope in the transmission mode. Parallel observations have been made using established X-ray and electron diffraction crystallographic techniques, Mössbauer effect and differential scanning calorimetry.

FORM 1473

UNCLASSIFIED

405 006

Abstract

The report describes the application of Lorentz electron microscopy to the study of structural changes of amorphous alloys in composition region $\sim Fe_{80}B_{20}$. Significant changes in the magnetic domain structure can in certain instances be associated with phase transitions, segregation and stress effects together with changes in the amorphicity. The appearance of magnetization ripple and the formation of regular stripe domain patterns are examples of the magnetic structures which can be observed by defocussing the electron microscope in the transmission mode. Parallel observations have been made using established X-ray and electron diffraction crystallographic techniques, Mossbauer effect and differential scanning calorimetry.

Preface

Earlier reports have included an appraisal of scanning transmission electron microscopy as a technique in relation to conventional transmission electron microscopy (1977) and the application to the study of metallic glasses (1978).

In this final report we describe the application of Lorentz electron microscopy to the study of amorphous materials which since their development over the past few years have presented some problems in the determination of changes in their microstructure of a number of alloys. $Fe_{84}B_{16}$, $Fe_{80}B_{20}$ and $Fe_{76}B_{24}$ have been selected for this report.

The study of the amorphous state has taken on a greater significance in recent years with the developments of methods of producing in quantity, amorphous specimens of materials normally considered as crystalline; in particular some of the metals of industrial importance such as iron. Features such as the degree of the amorphicity, the extent of any structural orientation, the effect of stress are clearly of some importance in the structural analysis and assessment of these materials. The very fact of this amorphicity means that since some of the 'normal' techniques available in the examination of crystalline materials may be restricted or may not be available, it is important that use should be made of additional methods of approach. This report describes the application of Lorentz electron microscopy to this problem by the observation of the magnetic structure of some of the amorphous alloys of iron-boron.

The magnetic domain structure of a ferromagnetic material is intimately related to its physical dimensions and to the existence of anisotropic properties associated with features of atomic arrangements (crystal structure), microstructure or stresses. Different crystalline phases and, indeed, amorphous and crystalline phases are usually distinguished from each other by diffraction methods using X-rays, neutrons or electrons and

also, in some case, by metallographic observation.

Investigations using Lorentz electron microscopy have shown that the form of the magnetic domain structure, imaged simply by operating the electron microscope in a defocussed setting, can distinguish between crystalline phases at high resolution. In order to illustrate the technique without the complication of amorphicity we use a crystalline material - cobalt. Figure P1 shows a thin foil of polycrystalline cobalt where the image of the domain structure is seen as a set of black and white lines which originate in an "overlapping" of the magnetic domains and a delineation of the boundaries ("domain walls") between neighbouring domains. It is clear that the parallel array of lines in the hexagonal (h.c.p.) areas (marked H) form a different pattern to lines in the cubic (f.c.c.) areas (marked F) which in places meet each other at triple junction. Similar differences in domain pattern also occur, of course, as a function of temperature when a phase transformation occurs.

In contrast amorphous materials are non-crystalline and have a random atomic arrangement, at least at long range, and although isotropic magnetic properties might be expected observed magnetic domain structures would suggest, in general, the presence of anisotropies which are not associated with long range atomic order. This kind of information would not be readily available from diffraction measurements as the presence of compositional or structural changes at short range and any associated stresses are difficult to detect. This report describes the results of an investigation in which one of the objectives was to explore the sensitivity of electron microscope images of electromagnetic structures to such effects on annealing some amorphous alloys of iron. Such systems should exhibit suitably minor changes in their atomic arrangements during annealing and crystallization which may be of significance in their macroscopic behaviour.

1. Introduction

The purpose of this report is to describe and discuss the results of an electron microscope investigation of the magnetic domain structure and physical microstructure in some amorphous magnetic alloys rapidly quenched from the liquid. This particular choice of investigation is an extremely timely one and is pertinent to the general aim of this project in which a correlation between electromagnetic structures and microstructures at high resolution was sought.

Amorphous ferro magnetic alloys of the Metglas type[1] were chosen as subject material because subtle changes in atomic arrangements and crystallization behaviour occur on thermal relaxation and annealing. It was felt that, as in amorphous magnetic films deposited from the vapour phase, these changes would be accompanied by related transformations in the magnetic domain structure[2]. Also, it was hoped that the possibility that any changes in magnetic structure might be as equally sensitive as diffraction measurements to alterations in atomic arrangements and changes of phase could be tested on these materials. Previous investigations[3] suggested that this might be the case. In contrast to as-deposited amorphous materials, complications from microstructural inhomogeneities (i.e. density and, possibly, compositional fluctuations) are essentially avoided in these alloys quenched from the liquid phase.

In the main, attention has been concentrated on compositions of the type $Fe_{100-x}B_x$ and in particular, $Fe_{84}B_{16}$, $Fe_{80}B_{20}$ and $Fe_{76}B_{24}$. This choice from the general composition range $(Fe,Co,Ni)_{100-x}(B,P,C)_x$ affords as simple a chemical composition as possible and suggests an easily characterised crystallization behaviour.

This project is not only of fundamental interest, but the results obtained may be significant for the commercial application of these materials. In the melt spun ribbon form

(see § 2), they are approaching competitiveness with available crystalline materials in their electrical, mechanical, corrosion resistance and, especially, magnetic[4] properties. Alloys of the compositions listed above are of particular interest as they exhibit high magnetic saturation, low coercivity, good thermal stability and outstanding mechanical properties. Low field properties and magnetization behaviour are intimately connected with domain structure and its interaction with microstructural features.

Only a limited range of amorphous alloy compositions can be made by rapid solidification from the liquid. This range is generally centred round the eutectic composition $TM_{80}Me_{20}$ where the transition metal TM = Fe,Co,Ni,Cr etc. and the metalloid Me = B,P,C or Si. In addition the eutectic temperature is particularly low in these systems. Other factors, such as the viscosity of the melt and the tendency for the melt to undercool also prevent crystallization.

The discussion of correlated magnetic domain and microstructural changes in this report is augmented by information given by coercivity measurements (obtained by others) and some differential scanning calorimetry and Mossbauer measurements on our specimen material.

2. Specimen Preparation and Experimental Procedure

The melt-spun ribbons were fabricated at the G.E. Research and Development Laboratories by a single operation process. The requirement for rapid quenching ($10^6 Ks^{-1}$) controls the thickness of ribbon contained and, with present technology, this is of the order of 50μm giving a cross section of 2 or 3 mm by 50μm. The details of the spinning process are given elsewhere[5].

Thin foils for transmission electron microscopy were prepared by electropolishing to perforation a 2mm x 2mm piece

of ribbon in a commercical, automatic electropolishing apparatus (Struers Vickers Ltd.). A suitable electrolyte was found to be 90 parts glacial acetic acid and 10 parts perchloric acid (by volume) cooled to about 5°C. For differential scanning calorimetry small pieces (~ 4 mg in weight) were cut from the master ribbons and some magnetization and Mössbauer spectroscopy measurements, were carried out on similar pieces.

Electron microscopy and electron diffraction was carried out in J.E.O.L. 200A and AEI Kratos EM7 electron microscopes at 200 keV and 1 MeV respectively. Both instruments are equipped with in-situ heating stages for annealing experiments and can operate in the Lorentz mode. The 200A also has an in-situ magnetization stage which was used for several magnetization experiments on the thin foils. This equipment is capable of producing magnetizing fields of the order of 400 Oe. Differential scanning calorimetry measurements were obtained using a Du Pont 990 thermal analyser with DSC cell. Some Mossbauer experiments were performed on a constant-acceleration spectrometer (in conjunction with a 1024 multichannel analyser) at the Solid State Physics Laboratory, University of Groningen, Netherlands. The source used was Co^{57} in Pd matrix.

3. Results

In the following sections we describe the results of a study of the microstructural and related domain changes in annealed $Fe_{76}B_{24}$, $Fe_{80}B_{20}$ and $Fe_{84}B_{16}$ alloy specimens.

3.1 Microstructural changes during annealing

During dynamic annealing the images of $Fe_{84}B_{16}$ specimens suddenly show what at low magnification may be appropriately termed - a characteristic mottling (Fig. 1a). This may occur anywhere in the range 330 - 370°C depending upon the

heating rate and the annealing time at temperature. At higher magnification (Fig. 1b) the mottling is seen to mark the onset of crystallization and, as deduced from the diffraction pattern, represents the primary crystallization of α-iron (b.c.c.). This behaviour is consistent with previous work on high iron content alloys[6].

A not dissimilar change is seen in $Fe_{80}B_{20}$ alloys but crystallization starts at a higher temperature (350-420°C) for the same time of anneal. However, the formation of local regions of α-Fe takes place on a much coarser scale (Fig. 2). This primary crystallization of α-iron has not been reported in other published data on $Fe_{80}B_{20}$ alloys[5]. On the other hand it should be noted that differential scanning calorimetry plots for both $Fe_{84}B_{16}$ and $Fe_{80}B_{20}$ (see § 3.5) show exotherms with a shape precisely as seen in other investigations[7]. The sequence of transformation in $Fe_{76}B_{24}$ alloy is similar, but the precipitated amount of αFe (Fig. 3) is very small compared with $Fe_{84}B_{16}$ and $Fe_{80}B_{20}$ alloys. Also the crystallization takes place at a temperature (455°C) higher than in the other two compositions.

If specimens in this initial crystallization state are now annealed at a slightly higher temperature, a further marked change occurs. This step is characterized, by the formation of spherulites (Fig. 4). It is believed that the spherulites represent a eutectic crystallization of Fe_3B and α-Fe (or possibly a polymorphous crystallization of Fe_3B) which is initiated when the matrix reaches the stoichiometric composition $Fe_{75}B_{25}$. As is shown in Fig. 4 the spherulites and initial α-Fe nuclei co-exist. Diffraction patterns from the spherulites show clearly the presence of tetragonal Fe_3B (Appendix 1). The spherulites consist of a series of columns which diverge radially from their centre. Although discrete,

the columns have similar crystallographic orientation as indicated by the single crystal nature of the diffraction patterns. Bend extinction contours are visible in the spherulites.

If specimens are now raised in temperature the crystallization proceeds not by the formation of many new spherulites, but by the rapid growth of those already present. As they expand, the matrix with its α-Fe is consumed, until the whole specimen is crystalline.

3.1.1 Differential Scanning Calorimetry

This is a technique widely used on bulk specimens to investigate the crystallization process[8]. We have used the calorimeter on the as-received ribbons of $Fe_{84}B_{16}$ and $Fe_{80}B_{20}$ alloys. Both the alloys show exotherms with a shape characteristic of those obtained in other investigations[6]. However, unlike the $Fe_{84}B_{16}$ alloy, $Fe_{80}B_{20}$ does not have a shoulder at lower temperatures (Fig. 5) as a satellite to the main crystallization peak. As a technique DSC measures macroscopic properties and is therefore less sensitive to the onset of crystallization than the electron microscope. This feature, together with the requirement of thin specimens means that data obtained with the microscope is not always consistent with that reported on bulk samples.

3.1.2 Mössbauer Studies

Mössbauer spectroscopy[9] has been used to investigate the internal fields within the ribbon samples. The internal field is sensitive both to the distribution of iron, and its environment, in the specimen, and can therefore detect the degree of crystallinity. Figure 6[9,6] shows Mössbauer spectroscopy from two $Fe_{84}B_{16}$ specimens after heat treatment

for 5 minutes. It can be seen from the figure that the precipitated amount of α-Fe is dependent on the annealing temperature . The amount of α-Fe was estimated to be 2.5% for the specimen heat-treated at 673 K and 0.9% for the one which was heat-teated at 663 K. This result is consistent with that reported by Kemeny et al[10]. It should be noted that Mössbauer spectroscopy with its high sensitivity, is particularly useful for low temperature annealing behaviour of the glassy alloys. The structural changes at low temperatures are too slight to be detected by DSC.

3.2 Domain Studies

3.2.1 Virgin Foils

Virgin specimens of all the alloys examined show the same featureless microstructure (Fig. 7a), a consequence of their amorphous nature. The only notable exception has been in some $(NiFe)_{80}B_{20}$ specimens where a degree of crystallinity has been detected - this must be attributed to an imperfect fabrication procedure.

The amorphous nature of the specimens also imposes a characteristic remanent domain structure which is typical of all the compositions observed. The characteristic of the remanent domain structure may be summarized as follows:

(1) The magnetization is confined to the plane of the specimen and its direction is isotropic within that plane.

(2) Clearly observed domain walls including cross tie walls exist within the material.

(3) The domains are fairly large, of the order of tens of microns - except in the vicinity of cracks, edges and holes. In such areas the domain structure is more complicated, [11] and determined by local magnetostatic effects[15]. For example, flux closing domains may be observed which form to reduce magnetostatic energy.

(4) Within the domains there is no sign of magnetization dispersion, i.e. 'ripple' which precludes any variation in magnetization direction on the micron scale.

It should also be noted that there is no sign of maze or stripe domains which are frequently observed[12] in the as-received ribbons before electrolytic thinning. In summary the remanent domain structures are characterized by planar isotropy and are remarkably similar to those seen in large grain low-anisotropy crystalline materials, such as Perminvar (Fe:Co:Ni = 34:23:43). A series of micrographs illustrating the above features is shown in Fig. 7b-e.

3.2.2 Domain Observations on Annealing

No sensible changes in domain structure occur until a temperature is reached where nuclei of α-Fe begin to form in the matrix . At this juncture Lorentz microscopy shows magnetization ripple[13] in $Fe_{84}B_{16}$ and $Fe_{80}B_{20}$ alloys (Fig. 8). The wavelength of the ripple is ∿ 1μm and is seen in both alloys. However, there is no evidence of such ripple in $Fe_{76}B_{24}$ alloy.

Thereafter the domain structure of $Fe_{80}B_{20}$ and $Fe_{84}B_{16}$ specimens diverge significantly as the temperature is raised. Most spectacularly, at a temperature of 390°C in the latter, a somewhat irregular stripe[15] domain structure is seen to form over a wide area of the specimen (Fig. 9a). At a lower magnification (Fig. 9b) the stripe domains are observed to co-exist with main domain walls and their mutual orientation would indicate that the stripe domain pattern is of the type designated weak[14]. This implies that the magnetization oscillates in and out of the film plane. The wavelength of the oscillatory structure is ∿ 5000 Å. The presence of stripe domains implies the existence of some anisotropy perpendicular to the film plane. The origin of this anisotropy is discussed

below.

As the temperature of the specimen is raised to a value where spherulite formation is initiated the spherulites are found to contain no stripe domain (Fig. 9b). However the spherulites, while initially of single domain size, soon grow to a size where they do support a domain structure. As crystallization proceeds to its conclusion the specimens are observed to have a domain structure typical of large grain crystalline materials.

No stripe domains at all can be created in the lower iron content specimens, $Fe_{80}B_{20}$. As the temperature is raised the ripple persists but is gradually destroyed by the nucleation and growth of spherulites. The ultimate domain structure is therefore similar in the fully crystallized species of both alloys studied.

3.2.3. Field Experiments

The domain walls in virgin specimens may be moved easily by the application of dc fields within the microscope. However the fields required to obtain saturation are generally $\sim$ 10 Oe implying that the coercivity is probably about 3 Oe. This is a value considerably higher than that normally reported for as-received ribbon ($\sim$ 0.1 Oe) and the discrepancy must be mainly attributed to the thinness of the microscope specimens.

The specimens may also be a-c demagnetized in-situ but the remanent domain structure shows no notable characteristic other than those described previously in section 3.2.1.

The domain structures described above represent remanent configurations at high temperatures but magnetic fields have been applied in-situ to annealed specimens at room temperature. Some micrographs from a 'run' performed on a partially crystallized $Fe_{84}B_{16}$ film containing spherulites is shown in Fig. 10. As already stated the spherulites, while capable of

supporting domain walls (see A), do not contain stripe domains - these are confined to the matrix. The stripe domains are easily removed by application of a field in the appropriate direction (Fig.10c). A residual ripple is left within the matrix. It may be noted from Fig.10b that walls within the spherulite can also be moved easily. Apparently the presence of spherulites does not significantly increase the coercivity of the foil. When the field is removed the stripe domain structure is recovered although, of course, there are differences in detail due to hysteresis.

4. Discussion of Microstructural and Related Domain Features

The development of the crystallization mechanism is largely in agreement with previously reported results (apart from the primary crystallization of α-Fe in $Fe_{80}B_{20}$) and is consistent with the kinetics discussed by Herold et al[5].

The changes in domain structure (not previously reported) accompanying the annealing procedure are extremely interesting, especially the creation of magnetization ripple and the existence of stripe domains. Generally speaking the domain structure of any specimen is sensitive to its material properties and therefore the observation of domains can provide significant information about the microstructure which may not be obvious through other means, e.g. in the diffraction pattern. Thus the presence of ripple denotes magnetization dispersion and one likely cause of the dispersion is a random system of stresses set up in the specimens. Since the dispersion appears with the onset of primary crystallization it appears probable that this nucleation is associated with microstresses. The absence of ripple in virgin specimens indicates that there are either no fluctuations in magnetization direction associated with structural (i.e. atomic) disorder on a scale 0-20 Å or that, if present, any resultant flux changes are near the

effective resolution limit of Lorentz microscopy.

It has been noted that the ripple is produced in all alloy compositions except $Fe_{76}B_{24}$. The absence of ripplies in $Fe_{76}B_{24}$ is attributed to the very low amount of precipitated α-Fe and hence the lack of associated microstresses. The appearance of stripe domain structures is limited to one composition only. In fact the presence of a weak stripe structure, which of necessity requires some sort of perpendicular anisotropy, is somewhat problematic. It clearly depends on iron content and probably upon the nucleation density of the primary crystallization. This suggests that dense mottling, as seen in $Fe_{84}B_{16}$, might be accompanied by stress and/or structural changes, such as columnar growth or some other form of non-equiaxed growth, which can produce stripe domains. This unidirectional columnar growth and consequent domain structure is subsequently destroyed or transformed when spherulites nucleate and form an array of radially directed columnar cells.

Bending stresses will also be present in the films but are unlikely to be distributed in such a way as to give stripe domains over the large areas in which they are observed to occur. Moreover, since these stresses are present in all samples and the magnetoelastic constants of $Fe_{84}B_{16}$, $Fe_{80}B_{20}$ and $Fe_{76}B_{24}$ are not dissimilar[15], it is difficult to explain why, on this basis, the stripe domains do not occur in the $Fe_{80}B_{20}$ and $Fe_{76}B_{24}$ compositions.

It must be admitted that the partially crystallized specimens are inhomogeneous in many respects (e.g. composition, magnetization values, stresses etc) and to tie down the precise mechanism responsible for stripe formation will not be easy.

Whatever the physical conditions necessary for stripe domain (and ripple) formation, observation proves that they are destroyed by the nucleation and subsequent growth of

spherulites. This is not too difficult to conceive of, since rapid grain growth at elevated temperature produces a more homogeneous microstructure. (The presence of bend extinction contours testifies to this assertion). As a result the fluctuations in stress, composition etc. existing on a scale of 0.1 - 1μm are eliminated.

The magnetic properties of the spherulites, especially in their early stages of life, are of interest. Presumably, they are initially single domains and therefore likely to increase coercivity. However, unlike permanent magnets, where the end particles are found within a non-magnetic matrix, the matrix in FeB alloys is itself magnetic. This means the single domain particle size is fairly large (~ 1 μm) because the matrix and spherulite have magnetization values differing by only a modest amount. As a result the impact of these particles within the matrix is not too drastic as far as dynamic magnetization properties are concerned. It is suggested that the evidence presented in § 3.4 supports this conclusion.

5. Conclusions

The correlation between magnetic domain structure and the physical microstructure of some annealed amorphous $Fe_{100-x}B_x$ alloys has been investigated with electron microscopy. On account of their potential applications these materials can be properly described as electromagnetic structures.

The study has shown that dynamic annealing of the alloys does result in characteristic and reproducible changes in microstructure. Moreover these changes are then responsible for important and drastic changes in the domain structure. Some of the latter, e.g. the formation of stripe domains, are, to say the least unexpected, and not predicted by any current metallurgical/magnetic theories. The creation of a stripe

structure lends credence to the assertion that the domain structure can be just as sensitive as indicator as diffraction data of subtle microstructural variations. This we consider to be one of the values of Lorentz transmission microscopy.

While the work has been mainly confined to thin foils, the results are certainly not irrelevant to bulk material. It is true that weak stripe domain formation as found here is a thin film phenomenon, but there is no reason why some type of three dimension ripple dispersion should not occur in as-received Metglas ribbons. For higher iron content alloys the formation of ripple is observed at fairly low temperature ($\sim 300^{o}C$) which might pose problems in some technical applications of the material.

TABLE I

OBSERVED AND ACTUAL DATA FOR Fe_3B PHASE

BODY-CENTRED TETRAGONAL CELL

a = 8.64 Å , c = 4.28 Å

INDICES h k ℓ	INTERPLANAR SPACING (Å)	
	OBSERVED	ACTUAL
101	3.86	3.84
211	2.87	2.87
110	6.08	6.10

Appendix I

Identification of Fe_3B Phase

Fig. A1 shows a typical diffraction pattern observed using a high tilt goniometer facility of the microscope. The phase is unambiguously identified to be Fe_3B. The procedure followed is as below.

Interplanar spacing (d) is given by:

$$d = \frac{2 \lambda L}{D} \qquad \ldots\ldots\ (1)$$

where $2 \lambda L$ = camera constant

D = distance between spots on either side of the centre

Camera constant was determined using α-Fe matrix as a 'built-in' standard and its value was found to be 3.040 cm Å. Values of d-spacings were calculated from the relationship[1]. Table I shows the list of the observed and actual inter-planar spacings. From the table I , there is good agreement between the observed and actual values.

References

1 F. E. Luborsky, Invited paper, Proc. Intern. symp. Amorphous Magnetism, Troy, N.Y., Aug. 1976

2 P. J. Grundy, to be published in IEEE Trans. Mag.

3 R. S. Tebble, Private Communication

4 F. E. Luborsky, J. J. Becker and R. D. McCary, IEEE Trans. Magn. 11, 1644 (1975)

5 H. H. Liebermann and C. D. Graham Jr., IEEE Trans. Mag. 12, 921 (1976)

6 V. Herold and V Koster, Rapidly Quenched Metals III, 281 (1978) (Metals Society)

7 Ibid T. Kemeny, I. Vincze, B. Fogarassy and S. Argis, 291

8. Analytical Calorimetry, Ed. R. S. Porters, S. F. Johnson

9. I. Vincze, Sol. State Commun., 25, 689 (1978)

10. T. Kemeny, I. Vincze, Private Communication

11. T. Sukahara, T. Saloh and T. Tsushima, IEEE Trans. Mag. 14, 1022 (1978)

12. J. J. Becker, IEEE Trans. Mag. 11, 1326 (1975)

13. S. Tsukahara, J. Phys. Soc. Japan, 23, 189 (1967)

14. I. B. Puchalska, Acta Phys. Pol., 36, 589 (1969)

15. A.R. Bhatti, P.J. Grundy, G.A. Jones and R.S. Tebble "An electron microscope study of microstructural and related domain changes in annealed FeB amorphous alloys" presented at I.C.M. 79 Munich , to be published in J. Magnetism and Magnetic Materials.

Group Publications

Bhatti, A R, Grundy, P J, Jones G A and Tebble, R S "An electron microscope study of microstructural and related domain changes in annealed FeB amorphous alloys" presented at I.C.M. 79 Munich to be published in J. Magnetism and Magnetic Materials.

Grant, W A, Ali, A, Chadderton, L T, Grundy, P J and Johnson, E. Production of amorphous alloys by ion implantation in Rapidly Quenched Metals III, 63-72. The Metals Society 1978.

Grundy, P J, Ali, A, Christodoulides, C E and Grant, W A. Amorphous transition metal-metalloid alloy films prepared by ion implantation Thin Solid Films 58 253-258 (1979)

Jones, G A. Magnetic contrast in the scanning electron microscope: an appraisal of techniques and their applications J Mag Magn Matls 8 263-285 (1978)

Jones, G A and Puchalska, I B. The birefringent effects of magnetic colloid applied to the study of magnetic domain structures Phys Stat Sol (a) 51 549-558 (1979)

Kalvius, G M and Tebble, R S "Experimental Magnetism" 346 pp. John Wiley (1979)

Puchalska, I B, Jones G A and Jouve, H. A new aspect on the observation of domain structures in garnet epilayers J Phys D: Appl Phys 11 L175-L178 (1978)

Diagrams

Staff involved in research

R.S. Tebble Professor of Physics

P.J. Grundy Senior Lecturer in Physics

G.A. Jones Lecturer in Physics

A.R. Bhatti Research Officer

FIGURE P1 DOMAIN STRUCTURE IN A COBALT FOIL

1a

1b

FIGURE 1 MOTTLING DUE TO PRIMARY CRYSTALLIZATION OF -Fe IN $Fe_{84}B_{16}$ (DIFFERENT MAGNIFICATION)

FIGURE 2 MOTTLING IN $Fe_{80}B_{20}$

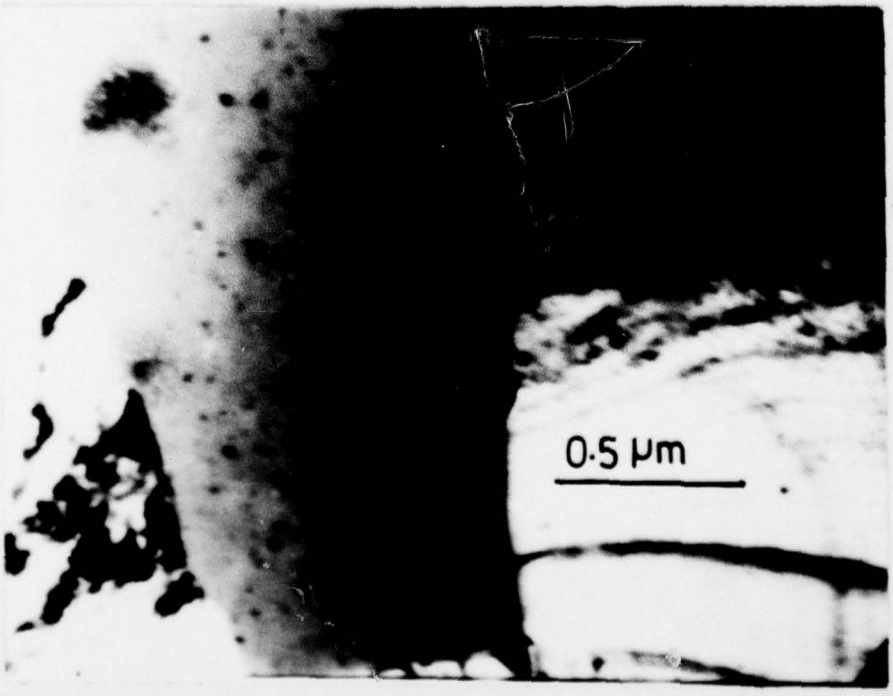

FIGURE 3 MOTTLING IN $Fe_{76}B_{24}$

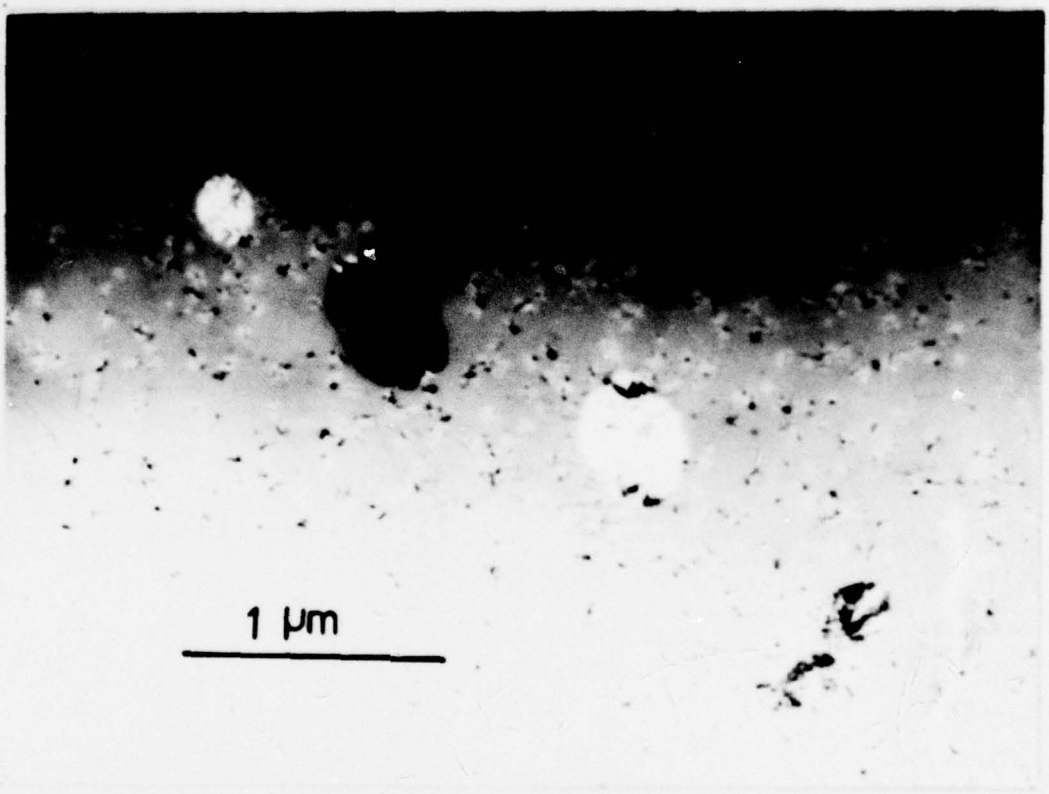

FIGURE 4 SPHERULLITE FORMATION IN $Fe_{80}B_{20}$

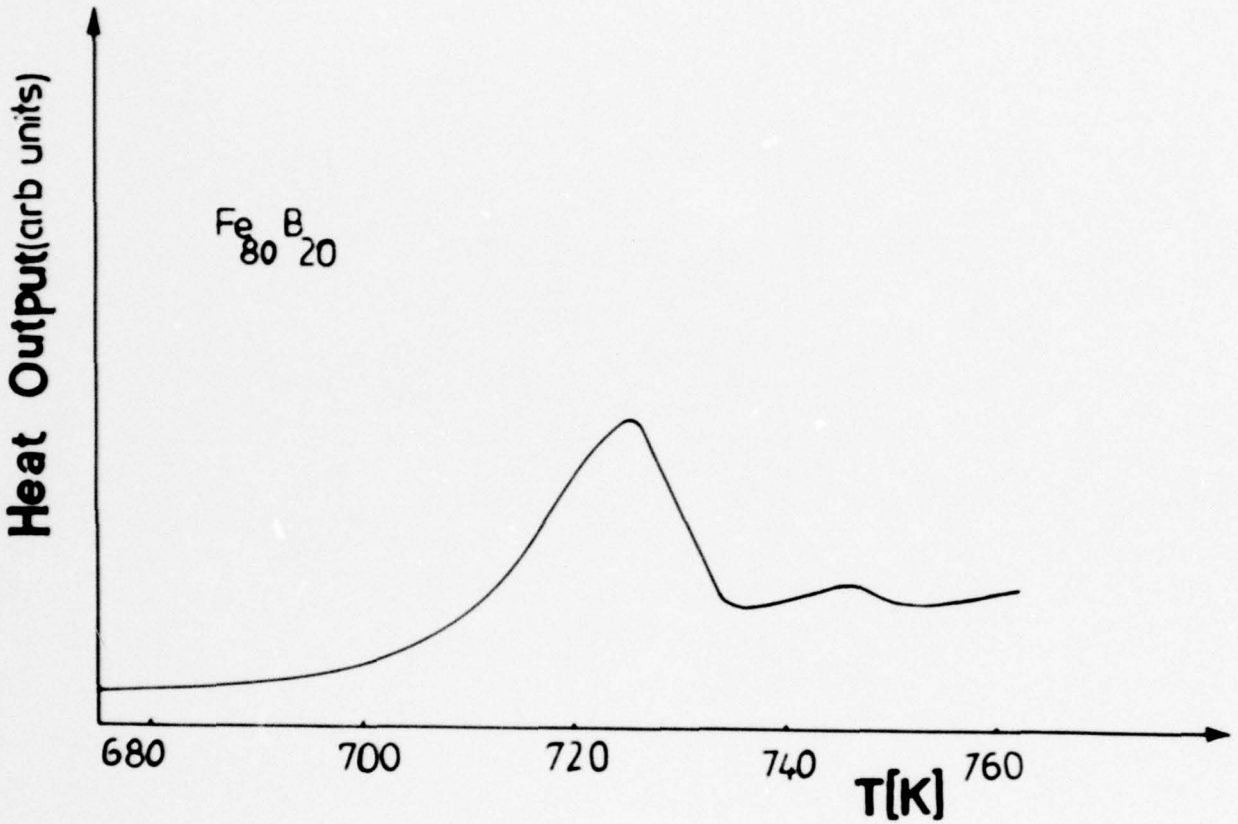

FIGURE 5A DIFFERENTIAL SCANNING CALORIMETRY PLOT OF $Fe_{80}B_{20}$

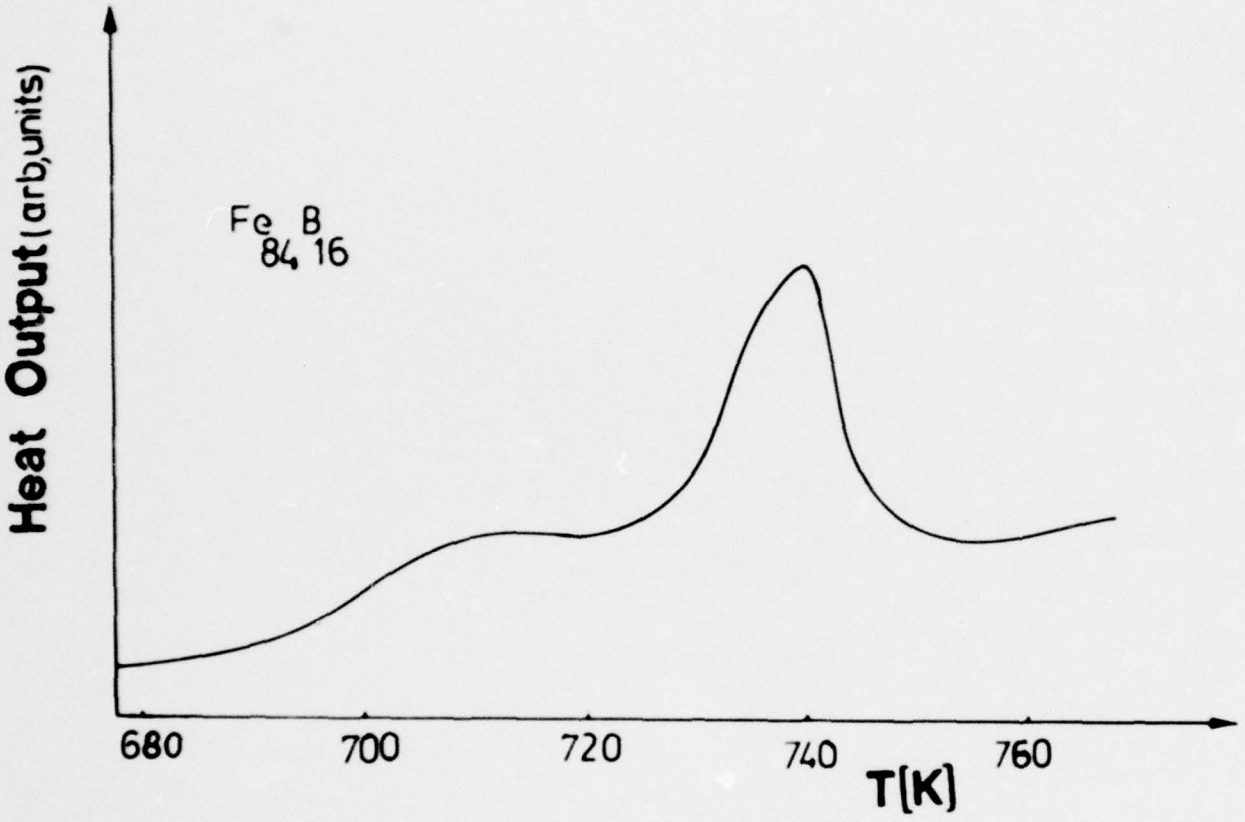

FIGURE 5B DIFFERENTIAL SCANNING CALORIMETRY PLOT OF $Fe_{84}B_{16}$

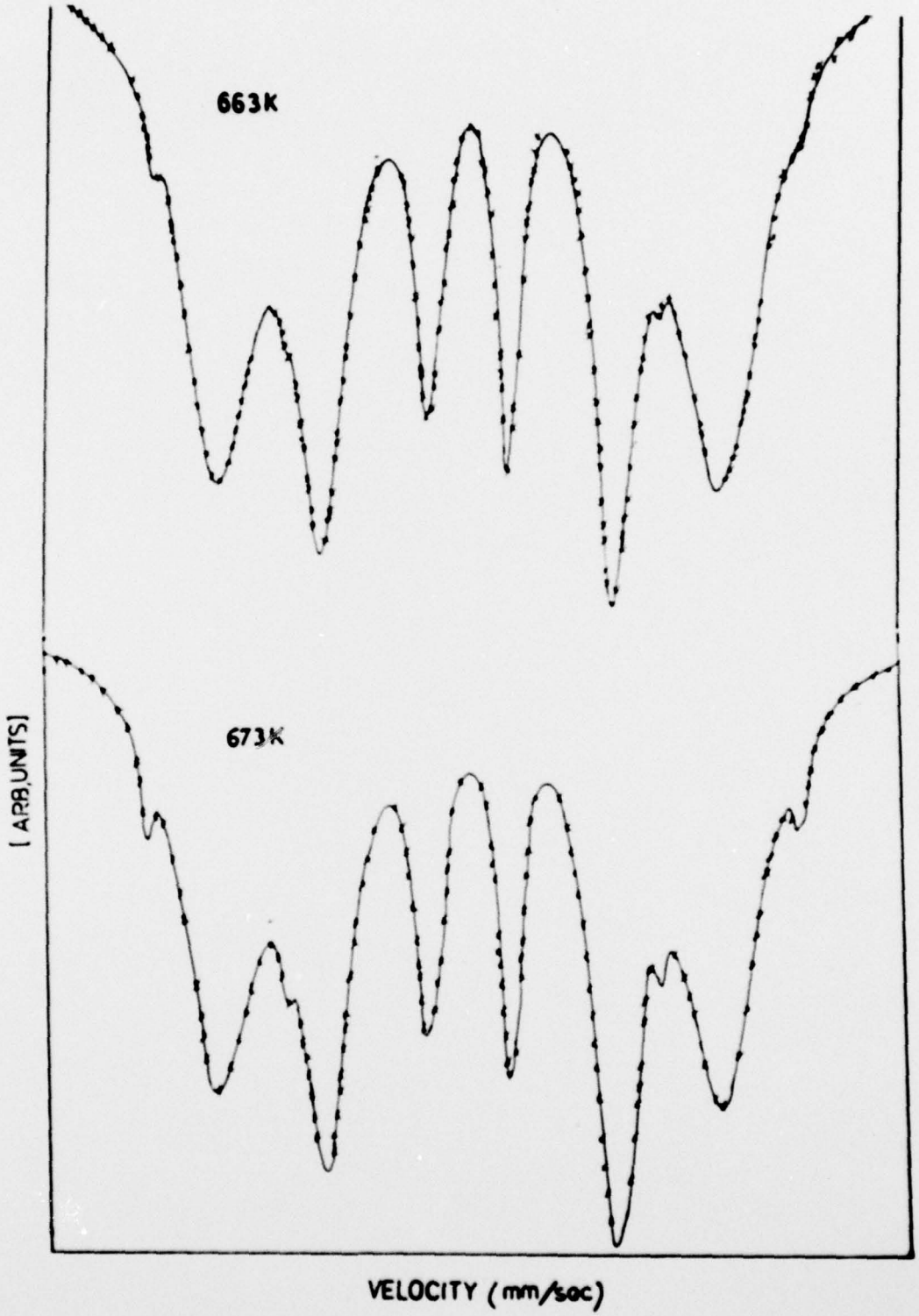

FIGURE 6 MÖSSBAUER SPECTRA OF $Fe_{94}B_{16}$

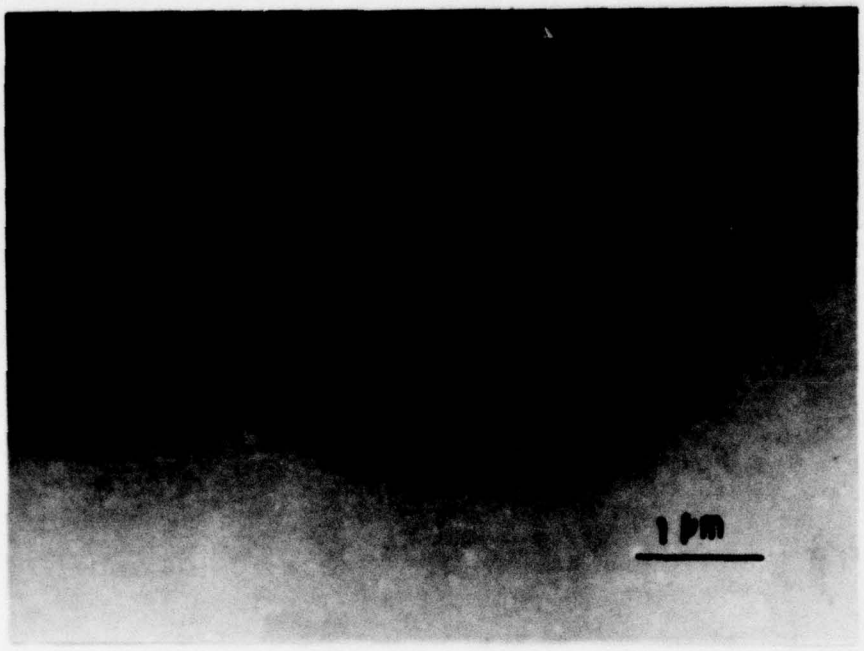

FIGURE 7A MICROSTRUCTURE OF AN AMORPHOUS FE-B VIRGIN FOIL

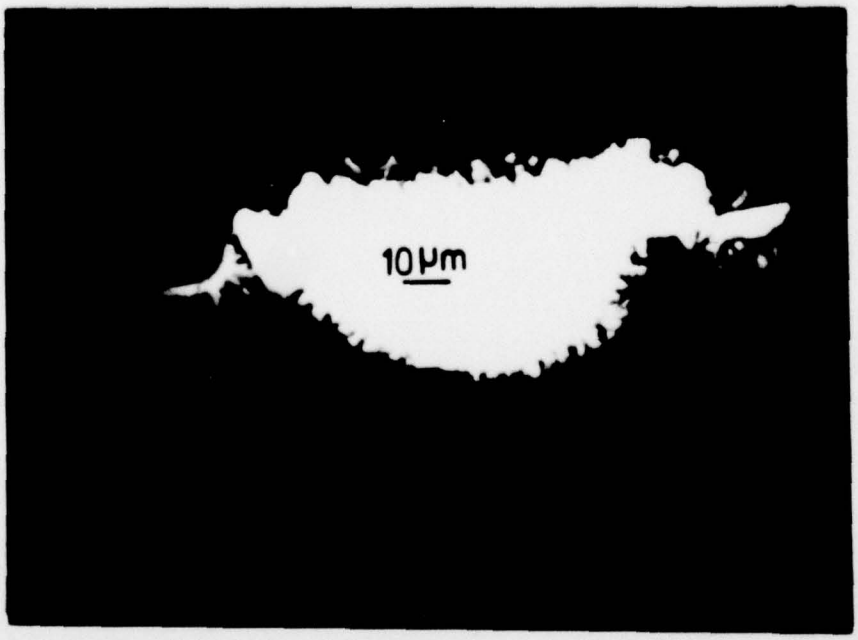

FIGURE 7B REMANENT DOMAIN STRUCTURE IN VIRGIN FEB FOILS

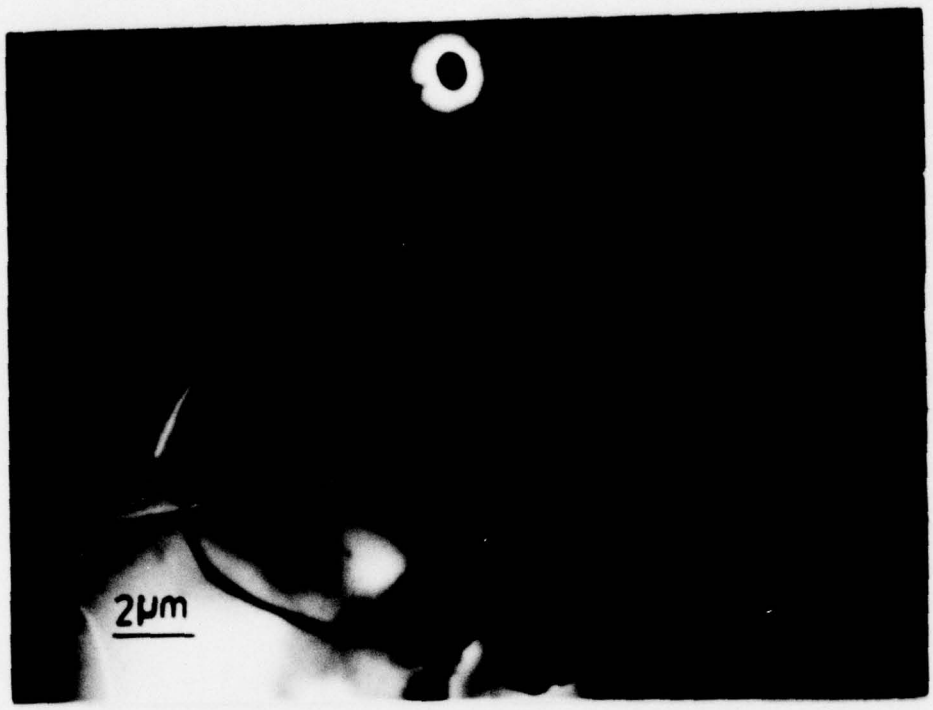

C

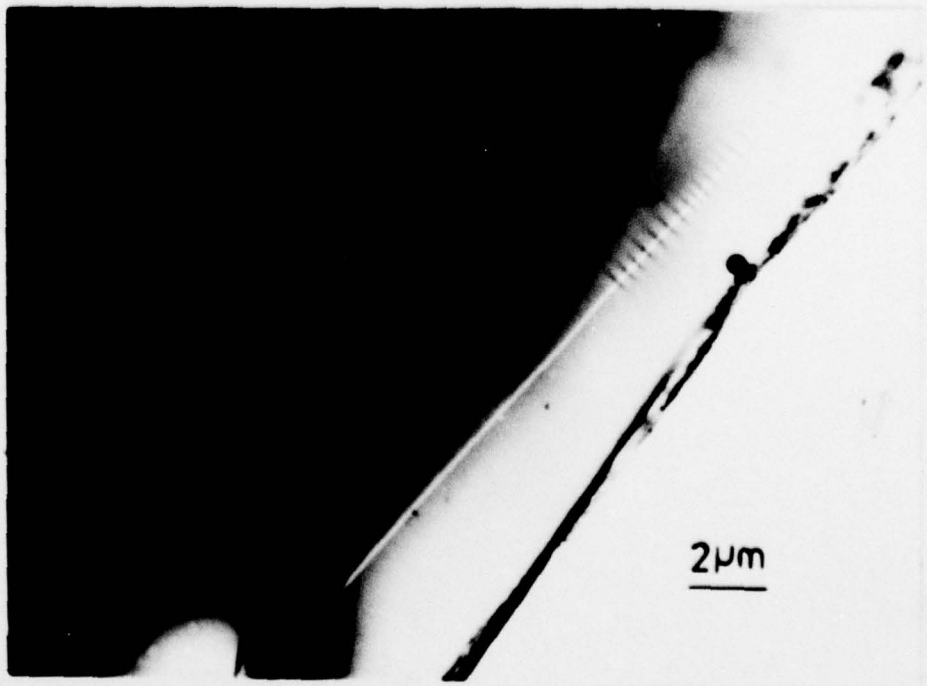

D

FIGURE 7 C&D REMANENT DOMAIN STRUCTURES IN VIRGIN FeB FOILS

FIGURE 7E REMANENT DOMAIN STRUCTURES IN VIRGIN FeB FOILS

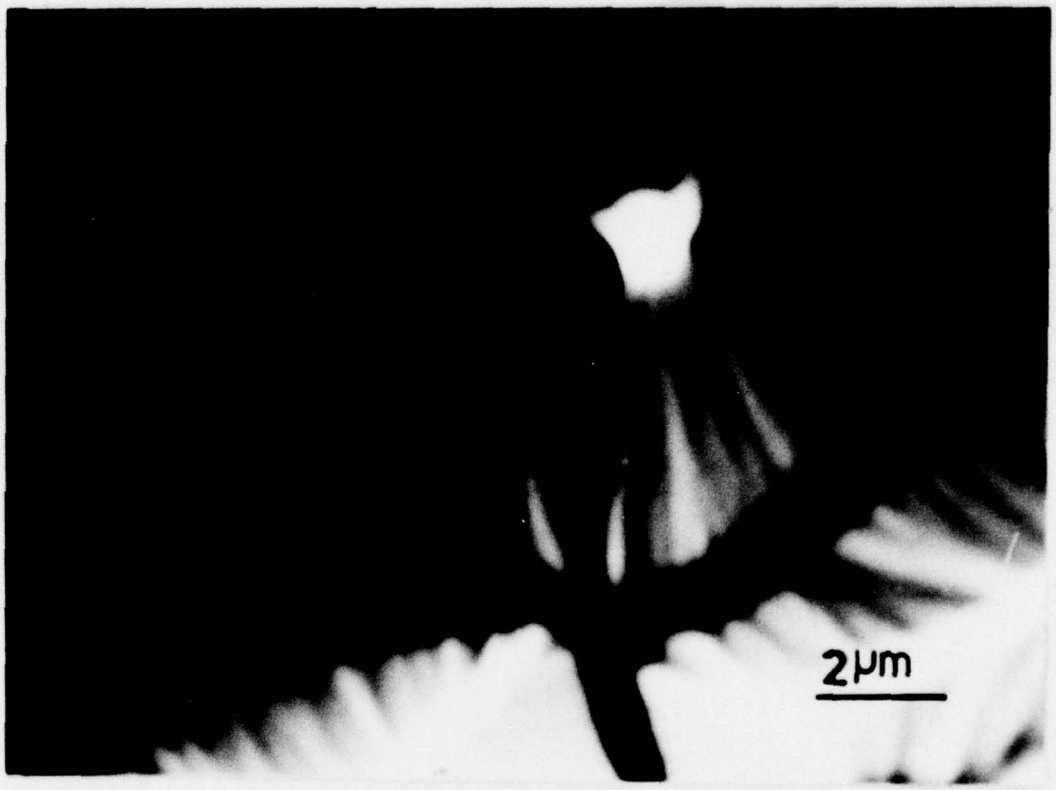

FIGURE 8 RIPPLE STRUCTURE IN ANNEALED $Fe_{84}B_{16}$

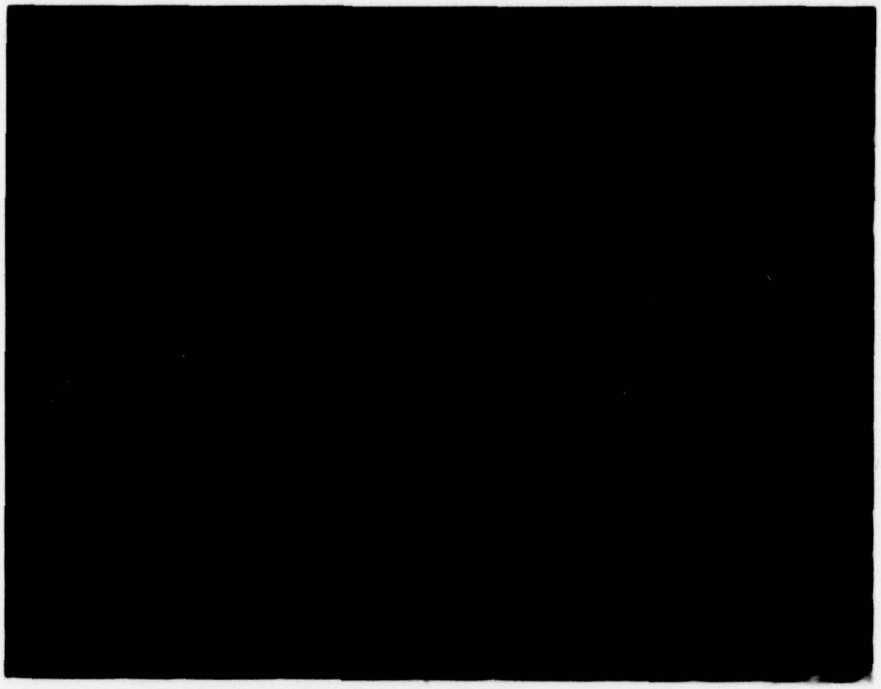

9A

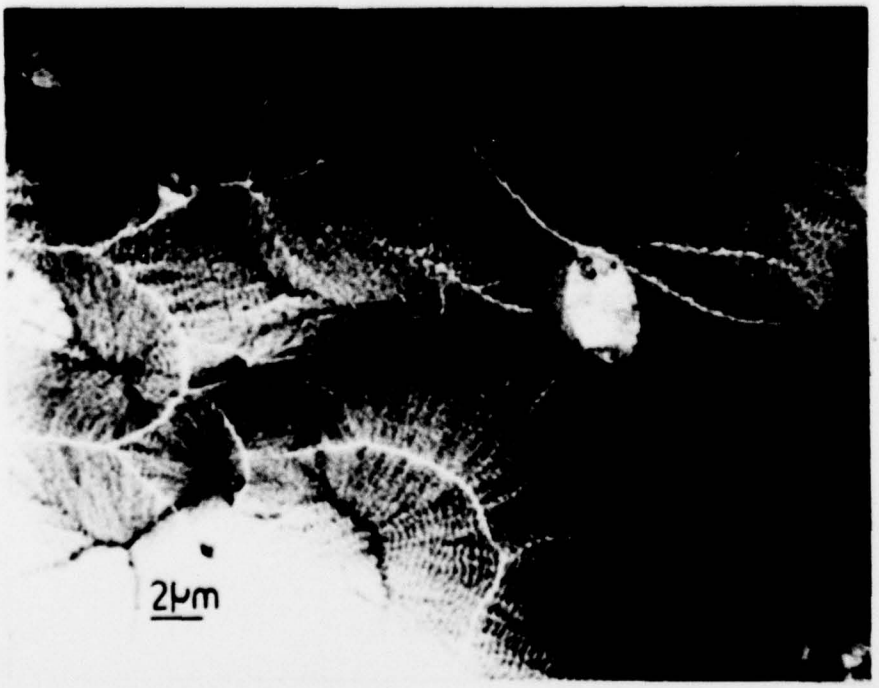

9B

FIGURE 9 A&B STRIPE DOMAINS IN ANNEALED $Fe_{84}B_{16}$

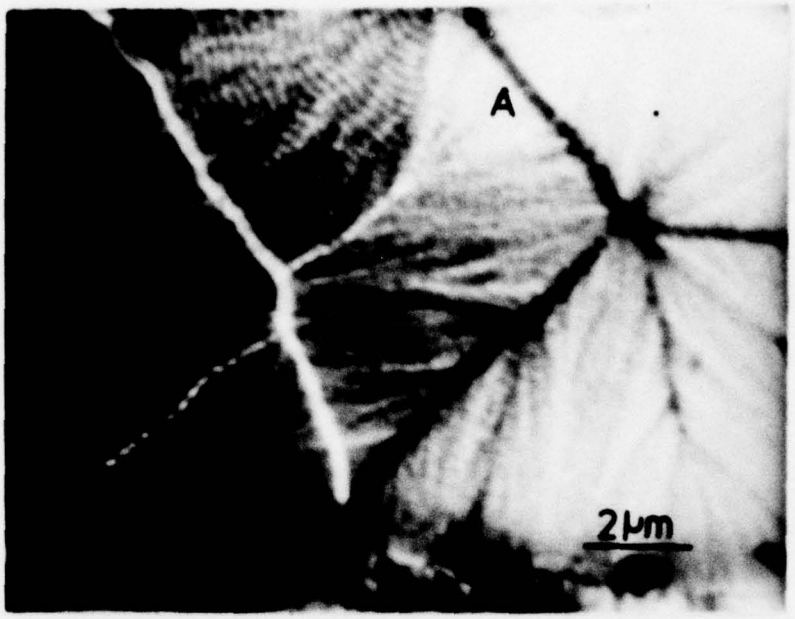

A

B

FIGURE 10A&B ANNEALED $Fe_{84}B_{16}$ FOIL IN AN APPLIED PLANAR FIELD (A) 0 OE (B) 60E

C

D

FIGURE 19 C&D ANNEALED $Fe_{84}B_{16}$ FOIL IN AN APPLIED PLANAR FIELD (C) 10 OE (D) 16 OE

E

F

FIGURE 10 E&F ANNEALED $Fe_{84}B_{16}$ FOIL IN AN APPLIED PLANAR FIELD (E) 6 OE (F) 0 OE

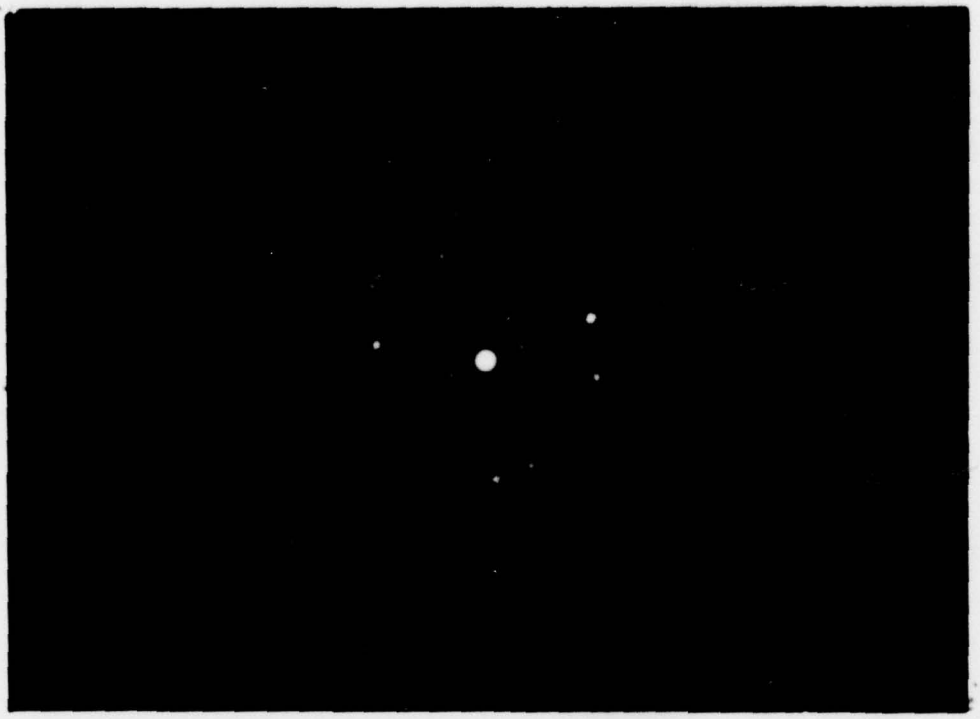

FIGURE A1 DIFFRACTION PATTERN FROM Fe_3B PHASE